

# Improved Electrochemical Performance of LaF<sub>3</sub>-coated Layered Oxide Li<sub>1.2</sub>Mn<sub>0.54</sub>Ni<sub>0.13</sub>Co<sub>0.13</sub>O<sub>2</sub> Cathode Material for Lithium-Ion Batteries Prepared by Sol-Gel Method

Le Wen, Zhijian Chang, Shuning Zhao, Jinli Liu, Zihao Zheng, Fengli Bei\*

China National Quality Supervision and Inspection Center for Industrial Explosive Materials, Nanjing University of Science and Technology, Nanjing, 210094, P.R. China.

\*E-mail: [beifl@njust.edu.cn](mailto:beifl@njust.edu.cn)

Received: 18 November 2020 / Accepted: 7 January 2021 / Published: 31 January 2021

---

In this article, the original Li<sub>1.2</sub>Mn<sub>0.54</sub>Ni<sub>0.13</sub>Co<sub>0.13</sub>O<sub>2</sub> lithium-rich manganese-based cathode material with a uniform distribution of polygonal prisms was synthesized by a simple and reproducible sol-gel method, followed by a simple chemical deposition method. The structure and electrochemical performance of the original and modified cathode materials were characterized by XRD, XPS, EDS, SEM, TEM, and constant current charge/discharge tests. The results showed that LaF<sub>3</sub> was uniformly coated on the surface of the original material and the thickness of the 2 wt% coating layer was about 2-3 nm. With this coating amount, the cathode material could obtain the best cycling and rate performance. The first coulomb efficiency of the modified material was 73%, which was 7% higher than that of the original material. Secondly, the cycling performance was improved. When the coated material was cycled at 0.2 C for 50 cycles, the discharge capacity was 325mAh·g<sup>-1</sup>, and the capacity retention rate was 99.21%, while the original material was only 78.73%. Finally, the performance was also improved at high current density. The coated material could still reach 170mAh·g<sup>-1</sup> at 5C, which was 70% higher than the original material. The significant improvement in electrochemical performance was attributed to the fact that the LaF<sub>3</sub> coating layer made the material avoid direct contact with the electrolyte which could reduce the occurrence of side reactions and increase the stability of the material. Besides, expanded layer space resulted from lattice expansion after coating could broaden the transmission channel of lithium ions and facilitate the insertion-extraction of lithium ions during charge and discharge.

---

**Keywords:** Li-ion battery Li<sub>1.2</sub>Mn<sub>0.54</sub>Ni<sub>0.13</sub>Co<sub>0.13</sub>O<sub>2</sub> Layered oxide Lanthanum fluoride Surface coating

## 1. INTRODUCTION

In order to solve the problem of environmental damage caused by over-exploitation of fossil fuels due to increasing energy demand of human, more and more renewable energy sources are discovered and used by humans, such as wind power, hydropower, and tidal power generation [1,2].

However, the use of these clean energy sources has problems that need to be solved urgently. These energy sources have periodic problems. They cannot be fully utilized when they are able to generate electricity and there will be a shortage of power supply when the conditions for generating electricity are not available. This requires high-performance power storage equipment. Secondly, people's growing material needs such as electric vehicles, wearable and portable smart devices also require rechargeable battery devices with high safety performance and strong endurance [3,4]. Commercially available batteries include  $\text{LiCoO}_2$  [5],  $\text{LiMn}_2\text{O}_4$  with spinel structure [6], and  $\text{LiFePO}_4$  with olivine structure [7]. However, their low battery capacity, poor safety performance during overcharge and low electrical conductivity severely limit the performance of fast charge and discharge. Therefore, people are concerned about batteries with large capacity, high safety, and wide window voltage that can be quickly charged and discharged. The layered lithium-rich manganese-based oxide which is usually expressed as  $x\text{Li}_2\text{MnO}_3 \cdot (1-x)\text{LiTMO}_2$  (TM = Mn, Co, Ni.) has become one of the most concerned cathode materials because it achieves a good balance among power, energy density, and cost [8,9].

The lithium-rich manganese-based cathode material  $x\text{Li}_2\text{MnO}_3 \cdot (1-x)\text{LiMO}_2$  (M=Ni, Co, Mn) is one of the most potential cathode materials for lithium-ion batteries. Its reversible specific capacity can reach  $250\text{mAh}\cdot\text{g}^{-1}$  and the working voltage up to 3.8 V and has a long cycle life, good thermal stability, easy preparation of materials, relatively low price, environmental friendliness and other excellent characteristics [10,11]. But there are also some unsolved problems. Among them, the irreversible capacity loss of the first charge caused by the mixing of cations is more serious. Under high charge and discharge voltage, the positive electrode material may react with the electrolyte solution and makes the cycle performance worse. The low lithium ion diffusion coefficient and electronic conductivity make the rate performance poor. The existence of these problems restrict its commercial application [12-14]. In response to the above problems, researchers modified the materials by surface coating, bulk doping and other means to achieve the purpose of improving electrochemical performance [15-17].

Surface coating modification has been experimentally proved to improve the electrochemical performance of lithium battery cathode materials under high cut-off voltage or more cycles. For example, Zhang et al. coated lithium-rich manganese-based cathode materials with lanthanum phosphate. The cycle stability of the modified materials was greatly improved and the capacity retention rate was as high as 83.2% after 200 cycles at 1C [18]. Besides, Chen et al. coated  $\text{Li}_{1.2}\text{Mn}_{0.54}\text{Ni}_{0.13}\text{Co}_{0.13}\text{O}_2$  cathode material with cerium phosphate, which increased the coulombic efficiency of the first turn from 88.26% to 92.19% and its performance at high temperature was also significantly improved, mainly due to the coating layer which can reduce the side reaction between the cathode material and the electrolyte and increase the diffusion channel of lithium ions [19].

In recent years, metal fluoride coating has a significant advantage in improving the electrochemical performance of cathode materials. The reason is that the metal fluoride coating layer can protect the cathode material from HF corrosion and the electronegative F can inhibit the transition metal migration to ensure the stability of the layered structure and to improve the cycle performance, voltage attenuation, and low first-lap coulomb efficiency. For example, Lu et al. reported that  $\text{Li}_{1.2}\text{Mn}_{0.54}\text{Ni}_{0.13}\text{Co}_{0.13}\text{O}_2$  cathode material with cerium fluoride coating has improved cycle and rate performance. Under 5C, the capacity increased from  $82.2\text{mAh}\cdot\text{g}^{-1}$  to  $103.1\text{mAh}\cdot\text{g}^{-1}$ . The reason is probably because the coating material suppresses the increase of impedance during the cycle [20]. In

addition, Niu et al. coated lithium-rich layered  $\text{Li}_{1.2}\text{Mn}_{0.54}\text{Ni}_{0.13}\text{Co}_{0.13}\text{O}_2$  cathode material with  $\text{YF}_3$  which greatly improved the high rate performance. The capacity increased from  $148.3 \text{ mAh}\cdot\text{g}^{-1}$  to  $179.6 \text{ mAh}\cdot\text{g}^{-1}$  at 5C. The reason is that in the process of  $\text{YF}_3$  modification and secondary baking, a spinel phase with three-dimensional  $\text{Li}^+$  diffusion channels is formed, which is beneficial to improve the rate performance [21].

In this article, the lithium-rich layered oxide  $\text{Li}_{1.2}\text{Mn}_{0.54}\text{Ni}_{0.13}\text{Co}_{0.13}\text{O}_2$  was first prepared by the sol-gel method and then a small amount of  $\text{LaF}_3$  was coated on the surface of the material by a simple chemical deposition method for modification. It was found that the rate performance, cycle performance, coulomb efficiency of the first charge and discharge and impedance performance of the material with a coating amount of 2% were significantly improved. In this paper, the reasons for the improvement of electrochemical performance were also deeply explored.

## 2. EXPERIMENTAL

### 2.1 Preparation of samples

The original layered oxide  $\text{Li}_{1.2}\text{Mn}_{0.54}\text{Ni}_{0.13}\text{Co}_{0.13}\text{O}_2$  powder was prepared by sol-gel method. First,  $\text{LiSO}_4\cdot\text{H}_2\text{O}$ ,  $\text{NiSO}_4\cdot 6\text{H}_2\text{O}$ ,  $\text{CoSO}_4\cdot 7\text{H}_2\text{O}$  and  $\text{MnSO}_4\cdot\text{H}_2\text{O}$  with a stoichiometric ratio of 1.26:0.13:0.13:0.54 were dissolved in deionized water to get a clear and transparent solution. Second, we weighed equimolar citric acid and dissolved it in a certain amount of deionized water. And then we added it dropwise to the metal salt mixed solution after the dissolution was completed. Third, we adjusted the pH of the solution to 8 with ammonia. The solution was placed in a water bath at  $85^\circ\text{C}$  and stirred until a gray wet gel was formed. It was then dried in a blast drying oven at  $120^\circ\text{C}$  for 12 h to form an off-white xerogel. After being fully ground, it was calcined by two stages ( $450^\circ\text{C}$ , 5h,  $850^\circ\text{C}$ , 12h) in an air atmosphere to obtain the original material.

In order to prepare  $\text{Li}_{1.2}\text{Mn}_{0.54}\text{Ni}_{0.13}\text{Co}_{0.13}\text{O}_2$  coated by  $\text{LaF}_3$ , the prepared raw material powder was added to the lanthanum nitrate ( $\text{La}(\text{NO}_3)_3$ ) aqueous solution under continuous stirring, and then the  $\text{NH}_4\text{F}$  aqueous solution was added dropwise to the suspension. The molar ratio of La to F was 1:3. Then, the suspension was stirred and evaporated in a water bath at  $80^\circ\text{C}$  until the water was completely evaporated. The dry powder was calcined in a tube furnace at  $450^\circ\text{C}$  for 5 hours in nitrogen atmosphere to obtain  $\text{LaF}_3$  coated  $\text{Li}_{1.2}\text{Mn}_{0.54}\text{Ni}_{0.13}\text{Co}_{0.13}\text{O}_2$  material. In this study, the coating amount of  $\text{LaF}_3$  on the original material was 1%, 2%, and 4%. The original material and the modified material were named Pristine, 1wt%- $\text{LaF}_3$ , 2wt%- $\text{LaF}_3$  and 4wt%- $\text{LaF}_3$  respectively.

### 2.2 Characterizations

The crystalline structure of samples was characterized by X-ray diffraction (XRD) using a Bruker D8 advance-X diffractometer with  $\text{Cu } \alpha$  radiation in the  $2\theta$  angular range of  $10^\circ$ - $80^\circ$  at a scanning rate of  $0.02^\circ/\text{s}$ . X-ray photoelectron spectroscopy (XPS, ESCALAB250) was performed to characterize the surface state of the obtained products. The particle morphology and element composition of the powders

were observed by using scanning electron microscope (SEM, USA JEM-1400plus) and energy dispersive spectroscopy (EDS). Transmission electron microscope (TEM, Japan JEM-1400plus) was used to examine the coating layer of cathode powders at an acceleration voltage of 80 kV.

### 2.3 Electrochemical measurements

First, polyvinylidene fluoride (PVDF), acetylene black and N-methylpyrrolidone (NMP) were mixed in a weight ratio of 8:1:1 then the active material was added. Then it was stirred overnight to form a uniform slurry. The obtained slurry was evenly coated on the aluminum foil, and it was placed in a blast drying oven at 120°C for 12 hours. After drying, it was cut into circular electrode sheets with a diameter of 16 mm using a punching machine. The battery assembly is operated in a glove box filled with argon gas. This study used the CR2016 button battery and high-purity lithium sheets as the negative electrode. The separator is a porous polypropylene film Celgard 2400 and the electrolyte is 1mol/L LiPF<sub>6</sub>/(EC+DEC+EMC) of which the volume ratio of EC (ethylene carbonate), DEC (diethyl carbonate), EMC (ethyl methyl carbonate) is 1:1:1. We use a sealer to seal the battery with a pressure of 50 MPa and let it stand for 12 hours. In this study, the button battery 3000-1 blue battery test system produced by Wuhan Lanbo Test Equipment Co., Ltd. was used to perform charge and discharge tests on the assembled CR2016 button battery. The test temperature is 25°C~30°C and the test voltage range is 2.0V-4.8V. Under 0.2C rate, charge and discharge cycle 50 times and carry out rate performance test at current density of 0.1C, 0.2C, 0.5C, 1C, 2C, 5C, 10C, where 1C=200 mA $h$ g<sup>-1</sup>. The CHI660C electrochemical workstation produced by Shanghai Chenhua Instrument Co., Ltd. was used to perform cyclic voltammetry and AC impedance testing on the assembled button battery. The cyclic voltammetry test temperature is 25°C~30°C, the scan rate is set to 0.1mV/s and the voltage range is 2.0V~4.8V. The AC impedance test conditions are: the test potential is 5mV, the frequency range is 0.01~100 000 Hz and the test temperature is 25°C~30°C.

## 3. RESULTS AND DISCUSSION

The XRD patterns of Li<sub>1.2</sub>Mn<sub>0.54</sub>Ni<sub>0.13</sub>Co<sub>0.13</sub>O<sub>2</sub> before and after LaF<sub>3</sub> modification were shown in Figure 1. The original materials and the materials synthesized with 1%, 2% and 4% LaF<sub>3</sub> coating amount all have characteristic peaks of the typical  $\alpha$ -NaFeO<sub>2</sub> structure. Secondly, there were some weaker diffraction peaks between 20°~25°, these diffraction peaks belong to the characteristic diffraction peak of Li<sub>2</sub>MnO<sub>3</sub> with monoclinic unit cell structure. It could also be seen from the figure that the (006)/(102) and (108)/(110) diffraction peak splitting degrees of the materials synthesized under LaF<sub>3</sub> coating amount were more obvious which indicated that the synthesized materials have relatively high complete layered structure. There was no characteristic diffraction peak of LaF<sub>3</sub> in the XRD pattern. This may be due to the low content of LaF<sub>3</sub> or the low sintering temperature during coating and the coating layer existed in an amorphous state without forming a crystal structure. Interestingly, the peak of the (104) crystal plane shifts to the left( 2 $\theta$  decreases) after LaF<sub>3</sub> coating. According to the Bragg equation,

$2d\sin\theta=\lambda$ ,  $d$  increases when the value of  $\theta$  decreases. It could be inferred that the coated material has undergone lattice expansion. This may be due to the fact that part of the  $F^-$  in the coating layer diffused into the bulk phase of the material due to the concentration gradient which increased the interlayer spacing. The increasing of the interlayer spacing made the insertion and extraction of  $Li^+$  easier and improved the  $Li^+$  transmission kinetics, which was beneficial to the improvement of rate performance.

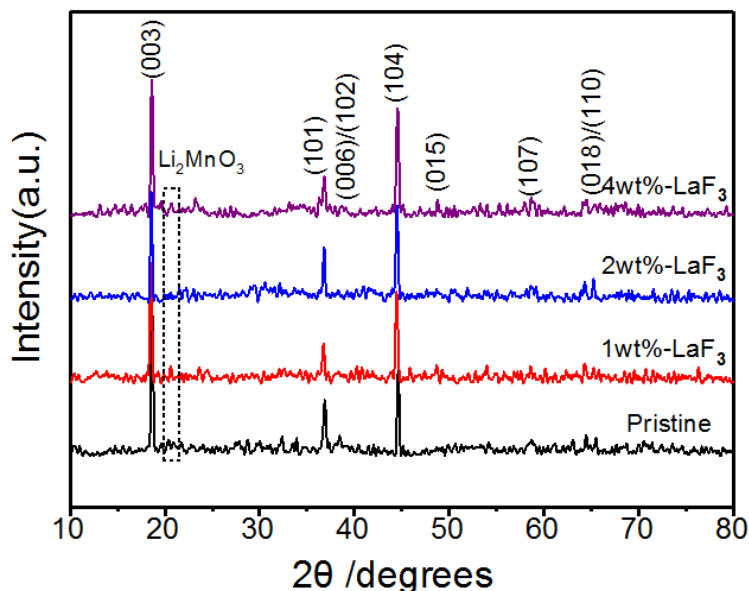


**Figure 1.** X-ray diffraction pattern of the Pristine, 1wt%-LaF<sub>3</sub>, 2wt%-LaF<sub>3</sub>, 4wt%-LaF<sub>3</sub>.

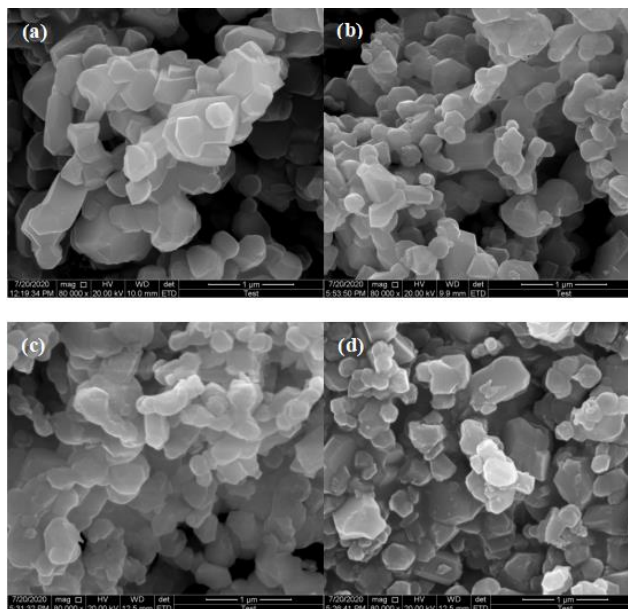
From the lattice parameters in Table 1, it could be seen that the parameters  $a$  of the materials coated with LaF<sub>3</sub> decrease first and then increase as the amount of coating increasing. The lattice parameter  $a$  usually represents the distance between transition metal atoms in the transition metal layer [22]. This might be due to the fact that a part of  $F^-$  ( $r=1.33\text{\AA}$ ) in the transition metal layer diffused into the bulk phase due to the concentration gradient, replacing  $O^{2-}$  ( $r=1.4\text{\AA}$ ) on the interface. It reduced the distance between the metal atoms in the transition metal layer. However, as the amount of coating increased, part of the transition metal might be reduced to a lower valence state due to the charge compensation of  $F^-$  substitution  $O^{2-}$  and the ion radius of the low oxidation state was larger than that of the high oxidation state [23]. The lattice parameter  $c$  usually represents the layer spacing [22]. We can see from Table 1 that the  $c$  value increased as the amount of coating increased indicating that the distance between the layers of the material has expanded. It could be calculated from Table 1 that when the coating amount was 2 wt%, the  $c$ -axis expansion rate reached 0.664%. It was consistent with the above-mentioned analysis. Besides, the unit cell parameters  $c/a$  of the materials were all greater than 4.899 indicating that the obtained materials all had a good layered structure. Except for 4wt%-LaF<sub>3</sub>, the  $I(003)/I(104)$  intensity ratio was greater than 1.2 indicating that the  $Li^+$  and  $Ni^{2+}$  cation mixing degree was very low [24]. As the coating amount increased, the  $I(003)/I(104)$  intensity ratio gradually decreased and part of the transition metal ions migrated into the Li layer causing mixed cations. When the coating

amount reached 4 wt%, the cation mixing was serious indicating that the coating amount should not exceed 4 wt%. The above analysis showed that the lithium-rich material synthesized by the sol-gel method had a good layered structure and the coating amount below 4 wt% did not change the crystal structure of the material.

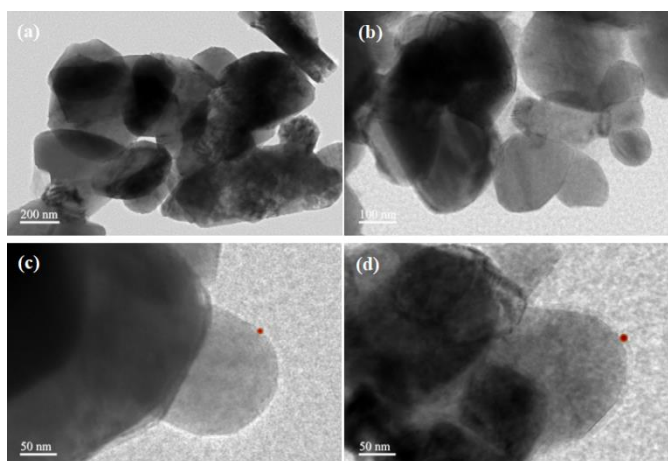
**Table 1.** The lattice parameters of four samples

Sample	a/Å	c/Å	c/a	I <sub>(003)</sub> /I <sub>(104)</sub>
Pristine	2.8582	14.3276	5.0128	1.6774
1wt%-LaF <sub>3</sub>	2.8485	14.3524	5.0385	1.3134
2wt%-LaF <sub>3</sub>	2.8604	14.4228	5.0422	1.2625
4wt%-LaF <sub>3</sub>	2.8612	14.4281	5.0426	1.1408

Scanning electron microscope (SEM) and transmission electron microscope (TEM) were used to study the morphology of the original raw materials and LaF<sub>3</sub> coated modified materials. As shown in Figure 2, all samples were polygonal and uniformly distributed with a diameter of 400-500 nm. Further observations showed that the particles grew uniformly and the surface was smooth and flat during the sol-gel synthesis process. But after LaF<sub>3</sub> modification, the surface gradually became rough. For 1wt%-LaF<sub>3</sub>, this change was not obvious due to less modification. For 2wt%-LaF<sub>3</sub>, the surface of the original material was covered with a uniform mesh coating layer. Such a structure provided a short path for the insertion/extraction of lithium ions which facilitated the transmission of lithium ions [25]. For 4wt%-LaF<sub>3</sub>, small particles of different sizes could be clearly seen on the surface indicating that the deposition of LaF<sub>3</sub> was uneven, which was caused by the accumulation of LaF<sub>3</sub> due to the excessive concentration of LaF<sub>3</sub>. This showed that the coating amount should be controlled reasonably. As shown in Figure 3, when the coating amount was 1 wt%, there was no obvious coating layer because the coating amount was too small [26]. When the coating amount was 2 wt% and 4 wt%, the coating thickness reaches 2-3 nm and 6-7 nm respectively. The coating layer was uniformly deposited on the surface of the original material. This thin coating layer would avoid direct contact between the electrode and the electrolyte, thereby reducing the side reactions between the active material and the electrolyte to a certain extent [27].

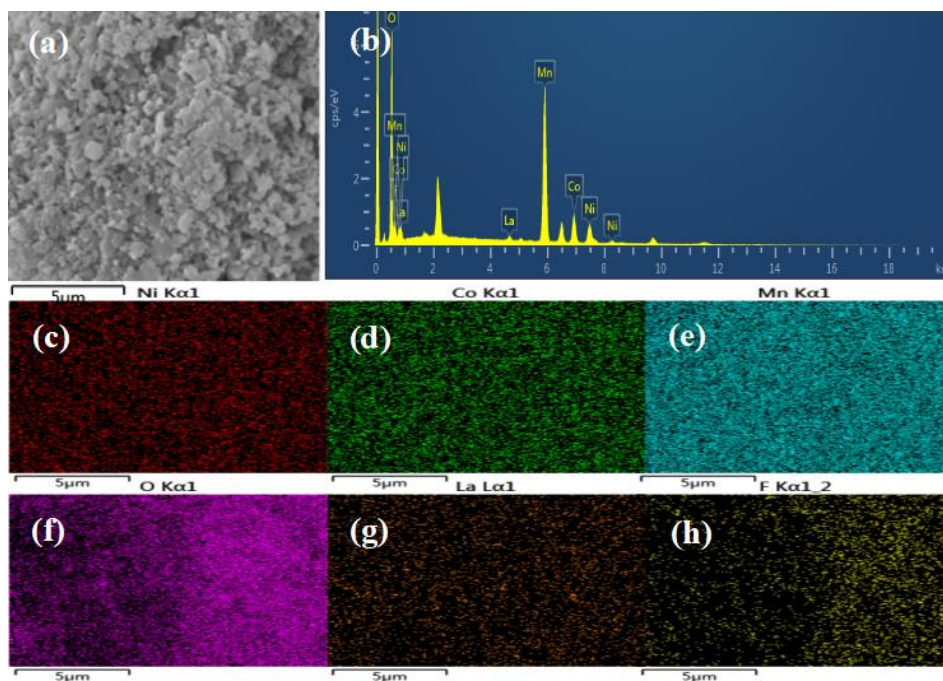


**Figure 2.** SEM images of prepared samples (a) Pristine, (b) 1wt%-LaF<sub>3</sub>, (c) 2wt%-LaF<sub>3</sub>, (d) 4wt%-LaF<sub>3</sub>.



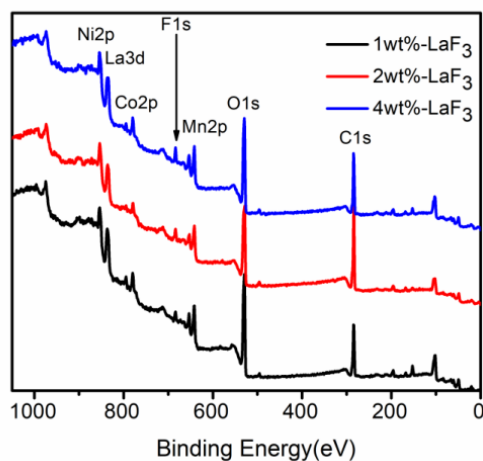
**Figure 3.** TEM images of prepared samples (a) Pristine, (b) 1wt%-LaF<sub>3</sub>, (c) 2wt%-LaF<sub>3</sub>, (d) 4wt%-LaF<sub>3</sub>.

In order to further observe the distribution of elements in the modified sample, we conducted EDS spectra in SEM mode [28]. EDS analysis (Figure 4) showed the presence of Ni, Co, Mn, F and La. The mapping of the sample coated with 2% LaF<sub>3</sub> (Figure 4c-4h) showed that F and La were uniformly distributed on the surface of the LNCMO particles. Therefore, the LaF<sub>3</sub> coating layer was evenly coated on the surface of the LNCMO material.

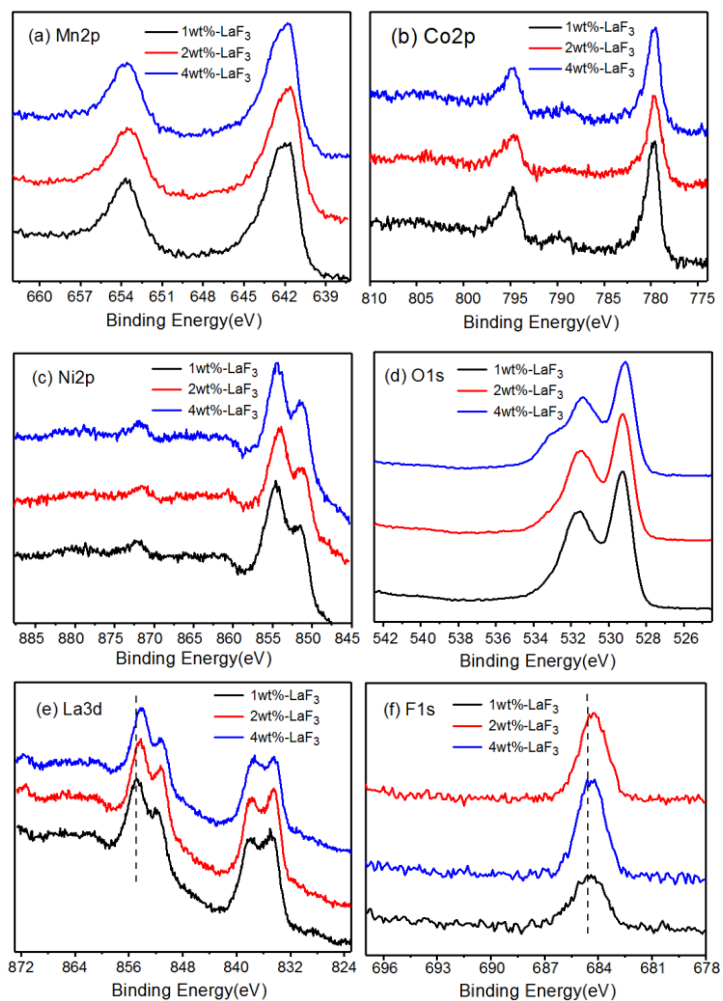


**Figure 4.** SEM image (a), EDS spectra (b) and the elemental mappings (c-h) of 2wt%-LaF<sub>3</sub> sample.

X-ray photoelectron spectroscopy (XPS) was used to study the surface composition of materials and the oxidation state of elements [29]. As shown in Figure 5, all coated modified samples exhibited characteristic peaks of F1s and La3d which confirmed the presence of LaF<sub>3</sub> coated on the surface. As shown in Figure 5 and Figure 6, the characteristic binding energies of F1s and La3d were 684 eV and 834.89 eV respectively which were consistent with the characteristic binding energies of pure LaF<sub>3</sub>. For materials with different coating amounts, the Ni2p and Mn2p peaks have no obvious chemical shifts which indicated that the Ni and Mn ion environment in the material structure has not changed. However, the F<sup>-</sup> binding energy moved to a low binding energy position as the amount of LaF<sub>3</sub> coating increases. This might be due to a part of F<sup>-</sup> diffusion into the bulk phase due to the concentration gradient replacing oxygen and binding with transition metal. It was beneficial to stabilize the material [30]. The result was consistent with the above-mentioned XRD analysis. Besides, the intensity of each peak of the coated material was reduced to different degrees which was attributed to the existence of the LaF<sub>3</sub> coating layer on the surface of the material. When the coating amount increased, the intensity of the F1s peak became significantly larger. Combined with XRD, EDS, XPS test results, we could confirm that LaF<sub>3</sub> was successfully coated on the surface of the original material.

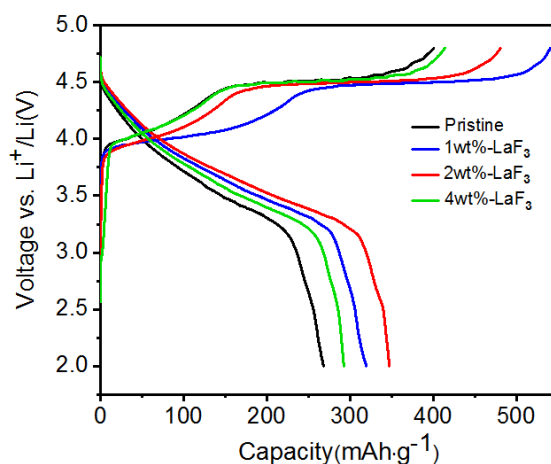


**Figure 5.** Chemical information for as-prepared materials with LaF<sub>3</sub> coating.



**Figure 6.** XPS spectra for Ni 2p, Co 2p, Mn 2p, O 1s, F 1s and La 3d.

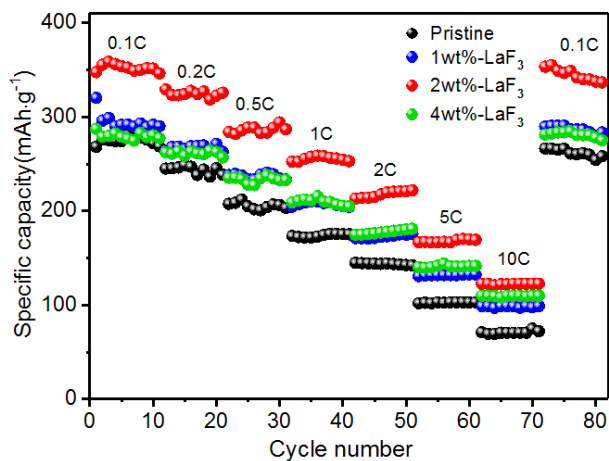
Figure 7 showed the first charge and discharge curves of Pristine and LaF<sub>3</sub> (1wt%-LaF<sub>3</sub>, 2wt%-LaF<sub>3</sub>, 4wt%-LaF<sub>3</sub>) coated modified materials at 0.1C. As shown in the figure, the discharge capacity of the unmodified sample was 265.0 mAh·g<sup>-1</sup> and the initial coulombic efficiency was 66.25%. The first coulombic efficiencies of the modified materials 1wt%-LaF<sub>3</sub>, 2wt%-LaF<sub>3</sub> and 4wt%-LaF<sub>3</sub> coated with LaF<sub>3</sub> were 58.3%, 73.0% and 65.8% respectively. The first irreversible capacities of Pristine, 1wt%-LaF<sub>3</sub>, 2wt%-LaF<sub>3</sub> and 4wt%-LaF<sub>3</sub> were 135 mAh·g<sup>-1</sup>, 225 mAh·g<sup>-1</sup>, 130 mAh·g<sup>-1</sup> and 140 mAh·g<sup>-1</sup> respectively. The results showed that coating the appropriate amount of LaF<sub>3</sub> (2wt%) on the lithium-rich manganese-based cathode material could effectively improve the initial coulombic efficiency of the lithium-rich cathode material and reduce the irreversible capacity loss during the first cycle which meant that the stability of the electrode structure has been greatly improved. The irreversible capacity loss was relatively low and the main reason for the high initial coulombic efficiency might be that the LaF<sub>3</sub> coating layer could be used as a protective layer to reduce the corrosion of the electrolyte on the material surface and inhibit the dissolution of transition metals [31].



**Figure 7.** The initial charge and discharge curves of Pristine, 1wt%-LaF<sub>3</sub>, 2wt%-LaF<sub>3</sub> and 4wt%-LaF<sub>3</sub> over 2.0-4.8V.

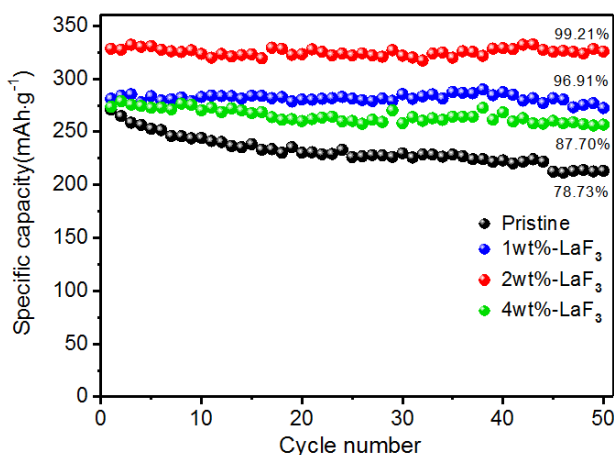
Figure 8 was the rate performance graph of four samples. The first charge and discharge were activated at the rate of 0.1 C (1C=200 mAh·g<sup>-1</sup>). The samples were charged and discharged for 10 cycles at 0.1C, 0.2C, 0.5C, 1C, 2C, 5C and 10C respectively. Finally, they were charged and discharged 10 cycles at 0.1C. It could be seen from Figure 8 that as the charge and discharge current increased, the discharge capacity gradually decreased. At the same time, it can be seen that the rate performance of all LaF<sub>3</sub> coated and modified materials have improved. However, the rate performance of the material with a coating amount of 2 wt% had the greatest increase. For example, the discharge capacity of 2wt%-LaF<sub>3</sub> at 1C was 260 mAh·g<sup>-1</sup>, while the original sample was only 165 mAh·g<sup>-1</sup>. The discharge specific capacity of the 2wt%-LaF<sub>3</sub> coated material at 5C is 170 mAh·g<sup>-1</sup>, which is 39.4% higher than the CeF<sub>3</sub> modified material (103.1 mAh·g<sup>-1</sup>) prepared by Lu [20]. In addition, when the current density returned to 0.1C, the discharge capacity could be fully recovered indicating that LaF<sub>3</sub> coated cathode material had

good electrochemical reversibility and structural stability. The increase in rate performance could be attributed to two reasons: (1) Parts of  $\text{La}^{3+}$  and  $\text{F}^-$  diffused into the bulk phase, XRD analysis showed that this would be conducive to the transmission of  $\text{Li}^+$ ; (2) The coating layer prevented the active material from directly contacting the electrolyte and stabilized the three-dimensional structure of the material [32].



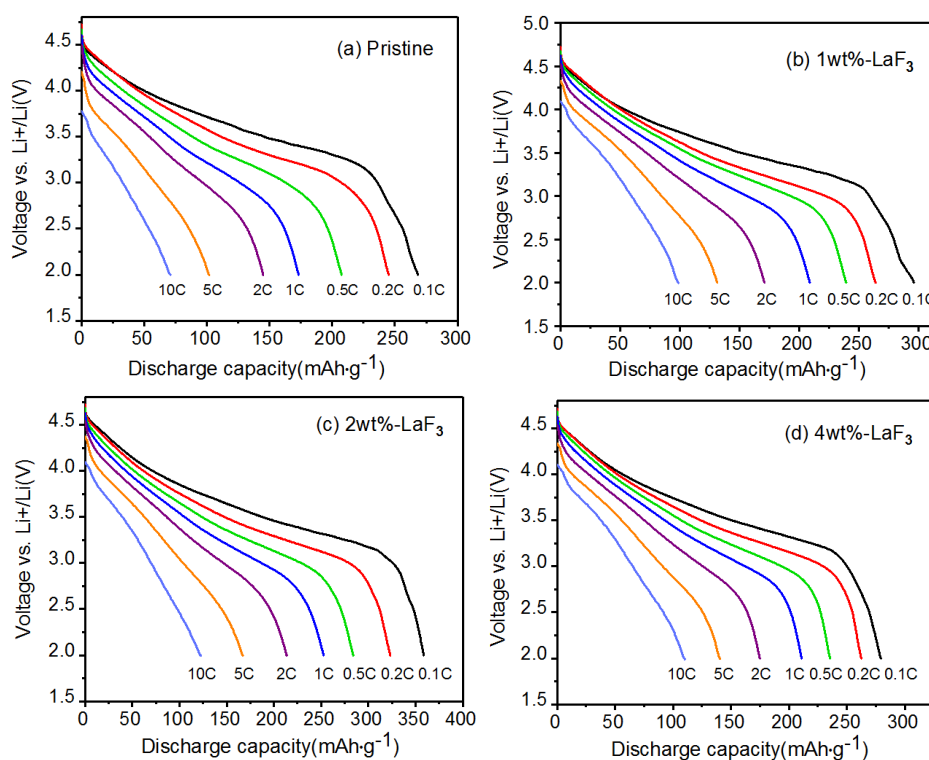
**Figure 8.** The rate performance for the Pristine, 1 wt%-LaF<sub>3</sub>, 2wt%-LaF<sub>3</sub>, 4wt%-LaF<sub>3</sub> respectively.

Figure 9 showed the cycle performance test of the four materials. The first cycles were activated at the rate of 0.1C and then they were charged and discharged at 0.2C and 2.0-4.8V for 50 cycles. The capacity of LaF<sub>3</sub> coated samples was higher than the original material. Secondly, compared with the original sample with a capacity retention rate of 78.73%, the capacity retention rate of the sample coated with 2 wt% LaF<sub>3</sub> remained stable at 99.21% after 50 cycles. The improvement in performance could be attributed to the LaF<sub>3</sub> coating which not only protected the electrode from the corrosion of the electrolyte but also stabilized the structure of the active material by reducing  $\text{O}^{2-}$  loss [33].



**Figure 9.** Cyclic performance of four samples during 50 cycles at a current density of 0.2C between 2.0 and 4.8V.

Figure 10 compared the rate performance of the four materials from 0.1C to 10C. Obviously, the LaF<sub>3</sub> coated sample showed better rate performance than the original sample. Among them, the material with 2 wt% coating had the best performance. As shown in Figure 10, the discharge capacity of the original material at current densities of 0.1C, 0.2C, 0.5C, 2C, 5C and 10C were 265.1 mAh·g<sup>-1</sup>, 248.2 mAh·g<sup>-1</sup>, 205.1 mAh·g<sup>-1</sup>, 175.3 mAh·g<sup>-1</sup>, 149.6 mAh·g<sup>-1</sup>, 105.3 mAh·g<sup>-1</sup> and 74.8 mAh·g<sup>-1</sup> respectively. In contrast, the discharge capacity of the material with 2 wt% coating were 355.1 mAh·g<sup>-1</sup>, 325.2 mAh·g<sup>-1</sup>, 280.1 mAh·g<sup>-1</sup>, 252.3 mAh·g<sup>-1</sup>, 215.6 mAh·g<sup>-1</sup>, 170.3 mAh·g<sup>-1</sup> and 125.8 mAh·g<sup>-1</sup>. Even at a high current density of 10C, the discharge capacity was still increased by 51 mAh·g<sup>-1</sup>. This fully showed that LaF<sub>3</sub> coated samples were more durable under high discharge current compared with uncoated modified materials and rate performance could be improved by surface modification with LaF<sub>3</sub> coating.



**Figure 10.** The initial discharge profiles of (a) Pristine, (b) 1wt%-LaF<sub>3</sub>, (c) 2wt%-LaF<sub>3</sub>, and (d) 4wt%-LaF<sub>3</sub> at a series of current densities.

Figure 11 showed the cyclic voltammetry curves of materials synthesized with different amounts of LaF<sub>3</sub> coating. It could be seen from the figure that the curves were consistent with the typical cyclic voltammetry curve of the lithium-rich cathode material [34]. In the first cycle, there were two obvious anode peaks which appeared in the voltage of 4.0~4.3V and 4.5~4.7V respectively. The first anode peak corresponds to the oxidation reaction of Ni<sup>3+</sup>/Ni<sup>4+</sup> and Co<sup>3+</sup>/Co<sup>4+</sup> accompanied by the release of Li<sup>+</sup> which corresponds to the first voltage plateau at the first charge. The second anode peak corresponds to the irreversibly release of Li<sub>2</sub>O from Li<sub>2</sub>MnO<sub>3</sub>, so the second anode peaks of the original material and the material with 1 wt% and 4 wt% coating amount disappeared in the last two scans. Interestingly, the

oxidation peak of the material with 2 wt% coating amount remained at 4.6V in the second circle which presumably because  $\text{Li}^+$  was not combined with  $\text{O}^{2-}$  after being released but reacted with the more electronegative  $\text{F}^-$  ions in the coating layer to form reversible  $\text{LiF}$ . Irreversible  $\text{Li}_2\text{O}$  was generated in the third cycle which was consistent with the charge-discharge curve. In addition, the cyclic voltammetry curves of the second circle and the third circle basically coincide after the first scan indicating that the electrode reaction was more reversible. But the first anode peak still had a small negative shift as the number of scan cycles increased. The peak intensity of the two cathode peaks gradually increased with the increased of the number of scanning turns. Especially the second cathode peak was the most obvious indicating that the material was further activated which was beneficial to the release of  $\text{Li}^+$  from the material. In addition, the peak of the cathode was about 3.8 V mainly due to the reduction of  $\text{Ni}^{4+}$  to  $\text{Ni}^{2+}$ .

Generally speaking, the cathode peak of 3.3 V will not appear in the initial discharge process [35,36], but a significant cathode peak appeared in the second and third cycles which indicated that the reduction of  $\text{Mn}^{4+}$  in layered manganese dioxide components resulted from the activation of electrochemical inactive component  $\text{Li}_2\text{MnO}_3$ . It showed the good reversibility of  $\text{Mn}^{4+}/\text{Mn}^{3+}$  redox reaction [37]. Compared with the 3.3 V cathode peak in the first cycle, these more pronounced cathode peaks in the second and third cycles indicated that  $\text{Mn}^{4+}/\text{Mn}^{3+}$  was easier to reduce after activating the  $\text{Li}_2\text{MnO}_3$  component in the first cycle.

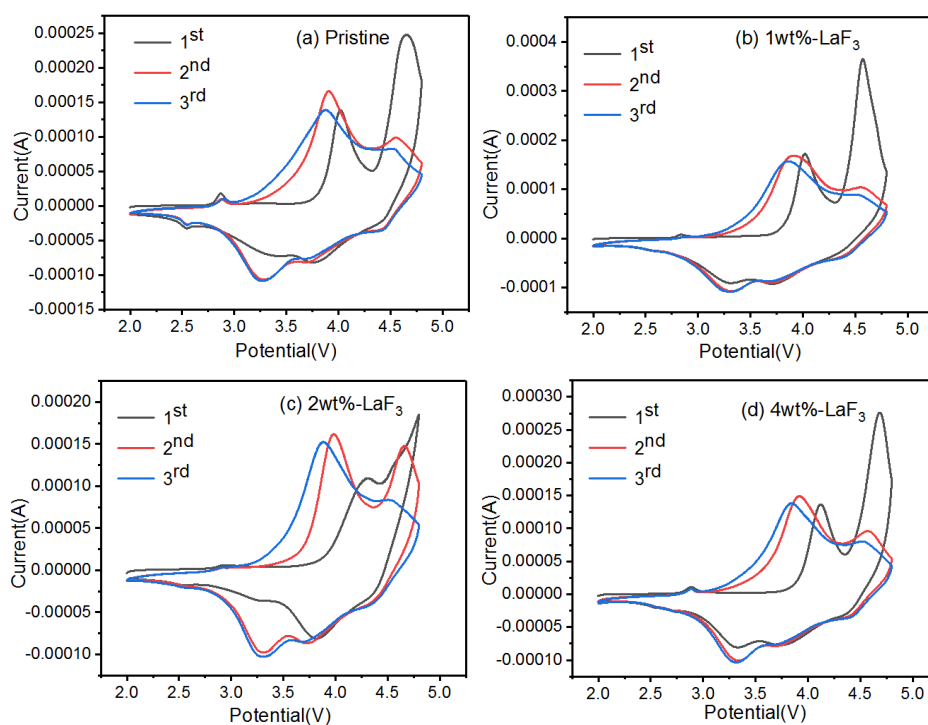


**Figure 11.** Cyclic voltammetry (CV) of (a) Pristine, (b) 1wt%- $\text{LaF}_3$ , (c) 2wt%- $\text{LaF}_3$ , (d) 4wt%- $\text{LaF}_3$ .

In order to understand the reasons for the improved performance of the LaF<sub>3</sub> modified material, the impedance spectra of the original material and the LaF<sub>3</sub> modified material were measured at a charging potential of 4.0V. It could be seen intuitively from Figure 12 that the AC impedance diagrams of all samples were composed of a semicircle in the high-frequency region and a diagonal line in the low-frequency region. The intersection of the starting point of the high-frequency region and the real axis was the solution impedance R<sub>E</sub> and the semicircle corresponded to the charge transfer resistance R<sub>ct</sub>. The diagonal line in the low frequency region represented the Warburg resistance of lithium ion diffusion [38]. The smaller the slope, the smaller the Warburg resistance. It could be seen from Figure 12(a) and Table 2 that the solution impedance of the material before and after coating did not change much and the charge transfer resistance of the original material was the highest at 121 Ω. The sample prepared when the coating amount was 2 wt% had the lowest charge transfer resistance which was 74.6 Ω. From Figure 12(b) and Table 2, it could be seen that the charge transfer resistance of the materials with the coating amount of 1 wt% and 2 wt% after 50 cycles were the smallest, about 44 Ω and the charge transfer resistance of the original material was the highest, about 80.5 Ω. It indicated that the coating can maintain a relatively stable structure and ions diffusion channel. The coating amount was too high (4wt%) which might cause certain damage to the material structure. Comparing Figure 12(a) and Figure 12(b), it could be seen that the impedance of the solution after 50 cycles was higher than that before the cycle. It might be caused by side reactions of the electrolyte under high voltage during the cycle and the charge transfer resistance of each material after the cycle became smaller than before the cycle which might be due to the activation of the material after the cycle. Secondly, the Warburg impedance of the material became larger after the cycle. This was because the layered structure of the material was corroded and phase change occurred after 50 cycles of the material which had an adverse effect on the diffusion of lithium ions [39]. In summary, among the four materials, the sample with 2 wt% coating had the smallest impedance indicating that the appropriate coating made the material structure more stable and improved the electrochemical performance.

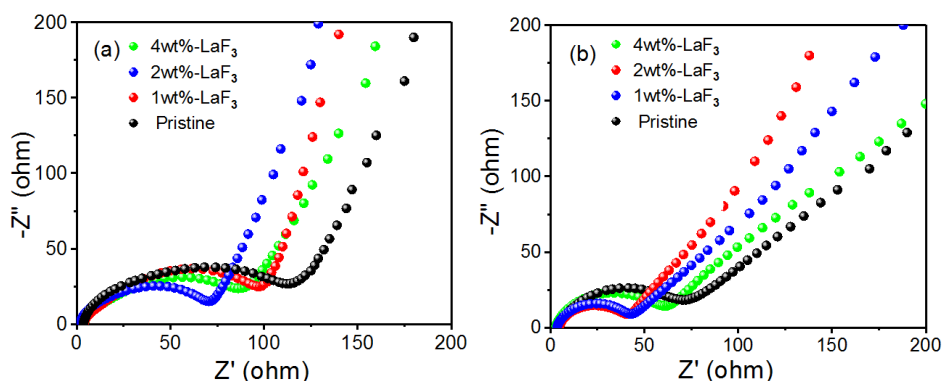


**Figure 12.** ESI spectrums of 0 (a) and 50<sup>th</sup> (b) for four sample.(in the charged stated of 4.0 V,1 MHz and 10MHz with an AC voltage of 5 mV).

**Table 2.** Resistance of 0 and 50<sup>th</sup> for four samples.

Sample	Pristine( $\Omega$ )	1wt%-LaF <sub>3</sub> ( $\Omega$ )	2wt%-LaF <sub>3</sub> ( $\Omega$ )	3wt%-LaF <sub>3</sub> ( $\Omega$ )
R <sub>E</sub> -0	3.6	3.5	3.3	3.8
R <sub>ct</sub> -0	121	110.8	74.6	98.3
R <sub>E</sub> -50	4.9	3.9	3.7	4.3
R <sub>ct</sub> -50	80.5	45.1	43.9	65.2

#### 4. CONCLUSION

In this paper, LaF<sub>3</sub> was successfully coated uniformly on the surface of lithium manganese base cathode material by chemical deposition method. The LaF<sub>3</sub> coating layer could effectively inhibit the side reaction between the cathode material and the organic electrolyte. In addition, lattice expansion occurred in the material after coating which widened the lithium ion transmission channel. It was conducive to the insertion and extraction of lithium ions and increased the migration rate of Li<sup>+</sup> at the interface. Thus, the electrochemical performance of the sample was significantly improved. In particular, the modified cathode material coated with 2 wt% LaF<sub>3</sub> had a higher coulombic efficiency (7%) than that of the original material due to the suppression of oxygen loss during the initial charging process and the discharge capacity was as high as 355.1 mAh·g<sup>-1</sup> at 0.1C. In addition, the LaF<sub>3</sub> coating layer could make the structure of the material surface more stable during charge and discharge. The 2 wt% LaF<sub>3</sub> coating modified cathode material had the best cycle performance and the capacity retention rate was 99.2% after 50 cycles at 0.2C. Therefore, we prepared the original material by the sol-gel method and successfully prepared the cathode electrode material with high electrochemical performance by the LaF<sub>3</sub> coating modification.

#### ACKNOWLEDGEMENTS

This work was partially supported by the National Natural Science Foundation of China (51472119 and 21474053) and A Project Funded by the Priority Academic Program Development of Jiangsu Higher Education Institutions (PAPD). Thanks support from China National Quality Supervision and Inspection Center for Industrial Explosive Materials, Nanjing University of Science and Technology.

#### References

1. Prasant Kumar Nayak, Evan M. Erickson, Florian Schipper, Tirupathi Rao Penki, Nookala Munichandraiah, Philipp Adelhelm, Hadar Sclar, Francis Amalraj, Boris Markovsky and Doron Aurbach, *Adv. Energy Mater.*, 8 (2018) 1702397.
2. John B. Goodenough and Youngsik Kim, *Chem. Mater.*, 22 (2010) 587.
3. Ming Xu, Linfeng Fei, Wei Lu, Zhaoyong Chen, Tao Li, Yan Liu, Guanyin Gao, Yanqing Lai, Zhian Zhang, Peng Wang and Haitao Huang, *Nano Energy*, 35 (2017) 271.
4. C. Zhan, T. Wu, J. Lu and K. Amine, *Environ. Eng. Sci.*, 11 (2018) 243.
5. W. Tang, L.L. Liu, S. Tian, L. Li, Y.B. Yue, Y.P. Wu, S.Y. Guan and K. Zhu, *Electrochem. Commun.*, 12 (2010) 1524.

6. Sen Zhao, Ying Bai, Qingjun Chang, Yuanqing Yang and Weifeng Zhang, *Electrochim. Acta*, 108 (2013) 727.
7. Youyong Liu, Chuanbao Cao and Jing Li, *Electrochim. Acta*, 55 (2010) 3921.
8. Arnaud J. Perez, Quentin Jacquet, Dmitry Batuk, Antonella Iadecola, Matthieu Saubanère, Gwenaëlle Rousse, Dominique Larcher, Hervé Vezin, Marie-Liesse Doublet and Jean-Marie Tarascon, *Nat. Energy*, 2 (2017) 954.
9. Shuai Liu, Xin Feng, Xuelong Wang, Xi Shen, Enyuan Hu, Ruijuan Xiao, Richeng Yu, Haitao Yang, Ningning Song, Zhaoxiang Wang, Xiaoqing Yang and Liquan Chen, *Adv. Energy Mater.*, 8 (2018) 1703092.
10. Jun Liu, B. Reeja-Jayan and Arumugam Manthiram, *J. Phys. Chem. C*, 114 (2010) 9528.
11. J. Gao, J. Kim and A. Manthiram, *Electrochemistry Communications*, 11 (2009) 84.
12. Abbas Fotouhi, Daniel J. Auger, Karsten Propp, Stefano Longo and Mark Wild, *Renewable Sustainable Energy Reviews*, 56 (2016) 1008.
13. Languang Lu, Xuebing Han, Jianqiu Li, Jianfeng Hua and Minggao Ouyang, *Journal of Power Sources*, 226 (2013) 272.
14. Jang Wook Choi and Doron Aurbach, *Nature Reviews Materials*, 1 (2016) 16013.
15. Meng Gu, Ilias Belharouak, Jianming Zheng, Huiming Wu, Jie Xiao, Arda Genc, Khalil Amine, Suntharampillai Thevuthasan, Donald R Baer, Ji-Guang Zhang, Nigel D Browning, Jun Liu and Chongmin Wang, *ACS Nano*, 7 (2013) 760.
16. S.J. Shi, J.P. Tu, Y.J. Zhang, Y.D. Zhang, X.Y. Zhao, X.L. Wang and C.D. Gu, *Electrochim. Acta*, 108 (2013) 441.
17. Xiaoyu Liu, Jali Liu, Tao Huang and Aishui Yu, *Electrochim. Acta*, 109 (2013) 52.
18. Tao Tao, Chao Chen, Yingbang Yao, Bo Liang, Shengguo Lu and Ying Chen, *Ceramics International*, 43 (2017) 15173.
19. J. J. Chen, Z. D. Li, H. F. Xiang, W. W. Wu, S. Cheng, L. J. Zhang, Q. S. Wang and Y. C. Wu, *RSC Adv.*, 5 (2015) 3031.
20. Chao Lu, Hao Wu, Yun Zhang, Heng Liu, Baojun Chen, Naiteng Wu and Sen Wang, *Journal of Power Sources*, 267 (2014) 682.
21. Xiaohui Zhang, Xin Xie, Ruizhi Yu, Jiarong Zhou, Yan Huang, Shuang Cao, Yu Wang, Ke Tang, Chun Wu and Xianyou Wang, *ACS Applied Energy Materials*, 2 (2019) 3532.
22. Siyu Liu, Zhilei Wang, Yongkui Huang, Zhijiang Ni, Jirong Bai, Shifei Kang, Yangang Wang and Xi Li, *Alloy. Comp.*, 731 (2018) 636.
23. L. Li, B.H. Song, Y.L. Chang, H. Xia, J.R. Yang, K.S. Lee and L. Lu, *J. Power Sources*, 283 (2015) 162.
24. Libin Gao, Zhengrui Xu and Shu Zhang, *Journal of Alloys and Compounds*, 739 (2018) 529.
25. Sung-Yoon Chung, Jason T. Bloking and Yet-Ming Chiang, *Nature Materials*, 1 (2002) 123.
26. Gang Li, Xu Chen, Yafei Liu, Yanbin Chen and Wensheng Yang, *RSC Advances*, 8 (2018) 16753.
27. Michael M. Thackeray, Sun-Ho Kang, Christopher S. Johnson, John T. Vaughey, Roy Benedek and S. A. Hackney, *Journal of Materials Chemistry*, 17 (2007) 3112.
28. Xingde Xiang, Xiaoqing Li and Weishan Li, *Journal of Power Sources*, 230 (2013) 89.
29. J.M. Zheng, X.B. Wu and Y. Yang, *Electrochimica Acta*, 56 (2011) 3071.
30. Jianming Fan, Guangshe Li, Dong Luo, Chaochao Fu, Qi Li, Jing Zheng and Liping Li, *Electrochimica Acta*, 173 (2015) 7.
31. Fuda Yu, Lanfang Que, Zhenbo Wang, Yuan Xue, Yin Zhang, Baosheng Liu and Daming Gu, *Journal of Materials Chemistry A*, 5 (2017) 9365.
32. Gang Wang, Liling Yi, Ruizhi Yu, Xianyou Wang, Yu Wang, Zhongshu Liu, Bing Wu, Min Liu, Xiaohui Zhang, Xiukang Yang, Xunhui Xiong and Meilin Liu, *ACS Applied Materials & Interfaces*, 9 (2017) 25358.
33. Hailin Zhang, Hongbin Zhao, Muhammad Arif Khan, Wenwen Zou, Jiaqiang Xu, Lei Zhang and

- Jiujun Zhang, *Journal of Materials Chemistry A*, 6 (2018) 20564.
34. Shengli Pang, Kaijie Xu, Yonggang Wang, Xiangqian Shen, Wenzhi Wang, Yanjing Su, Meng Zhu and Xiaoming Xi, *Journal of Power Sources*, 365 (2017) 68.
  35. Yang-Kook Sun, Min-Joon Lee, Chong S. Yoon, Jusef Hassoun, Khalil Amine and Bruno Scrosati, *Adv. Mater.*, 24 (2012) 1276.
  36. S.-H. Kang, Y.K. Sun and K. Amine, *Electrochem. Solid-State Lett.*, 6 (2003) A183.
  37. Shiyu Li, Xiaolan Fu, Youwei Liang, Jing Xie, Yuan Wei, Li Yang, Yamin Han, Wenbo Li and Xiaoling Cui, *Journal of Materials Science: Materials in Electronics*, 31 (2020) 5376.
  38. Hongming Zhou, Zhaohuim Yang, Chengjie Yin, Shengliang Yang and Jian Li, *Ceramics International*, 44 (2018) 20514.
  39. Zhongdong Peng, Kunchang Mu, Yanbing Cao, Lian Xu, Ke Du and Guorong Hu, *Ceramics International*, 45 (2019) 4184.

© 2021 The Authors. Published by ESG ([www.electrochemsci.org](http://www.electrochemsci.org)). This article is an open access article distributed under the terms and conditions of the Creative Commons Attribution license (<http://creativecommons.org/licenses/by/4.0/>).